Heat and mass transfer for Soret and Dufour's effect on mixed convection boundary layer flow over a stretching vertical surface in a porous medium filled with a viscoelastic fluid in the presence of magnetic field

By Gbadeyan, J.A., Idowu, A.S., Ogunsola, A.W., Agboola, O.O. , Olanrewaju, P.O.

Covenant University, Ota

Abstract - Thermal-diffusion and diffusion-thermo effects on combined heat and mass transfer on mixed convection boundary layer flow over a stretching vertical surface in a porous medium filled with a viscoelastic fluid in the presence of magnetic field is investigated. The partial differential equations governing the problem have been transformed by a similarity transformation into a system of ordinary differential equations which are solved numerically by using the shooting method with sixth-order of Runge-Kutta technique which are compared with Homotopy Adomian's Decomposition Method (HAM) for special case when magnetic field parameter is zero For fluids of medium molecular weight (H2, air), profiles of the dimensionless velocity, temperature and concentration distributions are shown graphically for various values of parameters embedded in the flow model. Finally, numerical values of physical quantities, such as the local skin friction coefficient, the local Nusselt number and the local Sherwood number are presented in tabular form.

Keywords : *Heat transfer; Soret effect: Dufour effect: Shooting method: viscoelastic fluid: magnetic field.*

GJSFR-A Classification : *FOR Code: 020404, 020304, 020303*

HEAT AND MASS TRANSFER FOR SORET AND DUFOURS EFFECT ON MIXED CONVECTION BOUNDARY LAYER FLOW OVER A STRETCHING VERTICAL SURFACE IN A POROUS MEDIUM FILLED

WITH A VISCOELASTIC FLUID IN THE PRESENCE OF MAGNETIC FIELD

Strictly as per the compliance and regulations of:

Open Association of Research, Soceity (Uinted States)

Heat and mass transfer for Soret and Dufour's effect on mixed convection boundary layer flow over a stretching vertical surface in a porous medium filled with a viscoelastic fluid in the presence of magnetic field

Gbadeyan, J.A.[α], Idowu, A.S.[Ω], Ogunsola, A.W.[β], Agboola, O.O.[ψ], Olanrewaju, P.O.[¥]

Abstract - Thermal-diffusion and diffusion-thermo effects on combined heat and mass transfer on mixed convection boundary layer flow over a stretching vertical surface in a porous medium filled with a viscoelastic fluid in the presence of magnetic field is investigated. The partial differential equations governing the problem have been transformed by a similarity transformation into a system of ordinary differential equations which are solved numerically by using the shooting method with sixth-order of Runge-Kutta technique which are compared with Homotopy Adomian's Decomposition Method (HAM) for special case when magnetic field parameter is zero For fluids of medium molecular weight (H_2, air), profiles of the dimensionless velocity, temperature and concentration distributions are shown graphically for various values of parameters embedded in the flow model. Finally, numerical values of physical quantities, such as the local skin friction coefficient, the local Nusselt number and the local Sherwood number are presented in tabular form.

Keywords : *Heat transfer; Soret effect: Dufour effect: Shooting method: viscoelastic fluid: magnetic field.*

I. INTRODUCTION

The problem of steady hydromagnetic flow and heat transfer over a stretching surface could be very practicable in many applications in the polymer technology and metallurgy. In particularly, many metallurgical processes involve the cooling of continuous strips or filaments by drawing them though a quiescent fluid and that in the process of drawing, these strips are sometimes stretched. In the case of annealing and thinning of copper wires, the properties of the final product depend to a great extent on the rate of cooling. By drawing such strips in an electrically conducting fluid subject to a magnetic field, the rate of cooling can be controlled and final products of desired characteristics might be achieved [1]. Also, in several engineering processes, materials manufactured by extrusions processes and heat treated materials traveling between a feed roll and a wind up roll on convey belts possess the characteristics of a moving continuous surface. The steady flow on a moving continuous flat surface was first considered by Sakiadis [2] who developed a numerical solution using a similarity transformation. Chiam [3] reported solutions for steady hydromagnetic flow over a surface stretching with a power law velocity with the distance along the surface. In many studies Soret and Dufour effects are neglected, on the basis that they are of a smaller order of magnitude than the effects described by Fourier's and Fick's laws. There are, however, exceptions. Eckert and Drake [4] have presented several cases when the Dufour effect cannot be neglected. Platten and Legros [5] state that in most liquid mixtures the Dufour effect is in operate, but that this may not be the case in gases. Benano-Molly et al. [6] have studied the problem of thermal diffusion in binary fluid, lying within a porous medium and subjected to a horizontal thermal gradient and have shown that multiple convection-roll flow patterns can develop depending on the values of the Soret number. They concluded that for saturated porous media, the phenomenon of cross diffusion is further complicated because of the interaction between the fluid and the porous matrix and because accurate values of the cross diffusion coefficients are not available. However, Soret and Dufour effects have been found appreciably influence the flow field in free convection boundary layer over a vertical surface embedded in a fluid-saturated porous medium.

Alan and Rahman [7], examined Dufour and Soret effects on mixed convection flow past a vertical porous flat plate with variable suction embedded in a porous medium for a hydrogen-air mixture as the non-chemical reacting fluid pair. Gaikwad et al. [8], investigated the onset of double diffusive convection in a two component couple stress fluid layer with Soret and Dufour effects using both linear and non-linear stability analysis. Emmanuel et al. [9] studied

Author [α ψ ¥] : Department of Mathematics, Covenant University, Ota. Ogun State. Nigeria.
Author [Ω] : Department of Mathematics, University of Ilorin, Nigeria.
Author [β] : Department of Pure and Applied Mathematics, Ladoke Akintola University of Technology, Ogbomoso.
E-mail : oladapo_anu@yahoo.ie

numerically the effect of thermal-diffusion and diffusion-thermo on combined heat and mass transfer of a steady hydromagnetic convective and slip flow due to a rotating disk with viscous dissipation and Ohmic heating. Anwar et al. [10] examined the combined effects of Soret and Dufour diffusion and porous impedance on laminar magneto-hydrodynamic mixed convection heat and mass transfer of an electrically-conducting, Newtonian, Boussinesq fluid from a vertical stretching surface in a Darcian porous medium under uniform transverse magnetic field. Nithyadevi and Yang [11] investigated numerically the effect of double-diffusive natural convection of water in a partially heated enclosure with Soret and Dufour coefficients around the density maximum. Recently, Olanrewaju [12] examined Dufour and Soret Effects of a transient free convective flow with radiative heat transfer past a flat plate moving through a binary mixture. Osalusi et al [13], investigated thermal-diffusion and diffusion-thermo effects on combined heat and mass transfer of a steady MHD convective and slip flow due to a rotating disk with viscous dissipation and Ohmic heating. Anwar Beg et al [14] examined the numerical study of a free convection magnetohydrodynamic heat and mass transfer from a stretching surface to a saturated porous medium with Soret and Dufour effects. Afify [15] studied the similarity solution in MHD: Effects of thermal diffusion and diffusion thermo on free convective heat and mass transfer over a stretching surface considering suction or injection. More recently, Hayat et al. [16], investigated heat and mass transfer for Soret and Dufour's effect on mixed convection boundary layer flow over a stretching vertical surface in a porous medium filled with a viscoelastic fluid.

The aim of this study is to investigate the steady mixed convection boundary layer flow due to the combined effect of heat and mass transfer over a stretched vertical surface in a porous medium filled with a viscoelastic fluid under Soret and Dufour's effects in the presence of magnetic field. It is interesting to note that Hayat et al. [16] is a special case in this present study. To the best of the author's knowledge, this problem has not been considered before.

II. MATHEMATICAL MODELS

We consider the heat and mass transfer flow due to stretching of a heated or cooled vertical surface of variable temperature $T_w(x)$ and variable concentration $C_w(x)$ in a porous medium filled with a viscoelastic fluid of uniform ambient temperature T_∞ and uniform ambient concentration C_∞. It is assumed that the surface is stretched in its plane with velocity $u_w(x)$. The density variation and the buoyancy effects are taken into consideration, so that the Boussinessq approximation for both the temperature and concentration gradient can be adopted. In addition the Soret and Dufour effects are considered in the presence of magnetic field. In the absence of heat generation and viscous dissipation, the steady boundary Layer equations are given by [17],

$$\frac{\partial u}{\partial x}+\frac{\partial v}{\partial y}=0, \tag{1}$$

$$u\frac{\partial u}{\partial x}+v\frac{\partial u}{\partial y}=\upsilon\frac{\partial^2 u}{\partial y^2}+k_0\left(u\frac{\partial^3 u}{\partial x\partial y^2}+\frac{\partial u\partial^2 u}{\partial x\partial y^2}+\frac{\partial u\partial^2 u}{\partial y\partial y^2}+\upsilon\frac{\partial^3 u}{\partial y^3}\right)-u\frac{\upsilon}{K}-u\frac{\sigma B_0^2}{\rho} \\ +g\beta_T(T-T_\infty)+g\beta_C(C-C_\infty), \tag{2}$$

$$u\frac{\partial T}{\partial x}+v\frac{\partial T}{\partial y}=\alpha_m\frac{\partial^2 T}{\partial y^2}+\frac{D_e k_T}{c_s c_p}\frac{\partial^2 C}{\partial y^2}, \tag{3}$$

$$u\frac{\partial C}{\partial x}+v\frac{\partial C}{\partial y}=D_e\frac{\partial^2 C}{\partial y^2}+\frac{D_e k_T}{T_m}\frac{\partial^2 T}{\partial y^2}. \tag{4}$$

The boundary conditions at the sheet (wall) and in the free stream are:

$$u=U_w(x)=ax, \quad v=0, \, T=T_w(x)=T_\infty+bx, \, C=C_w(x)=C_\infty+cx \, \, at \, \, y=0,$$

$$u\to 0, \, \frac{\partial u}{\partial y}\to 0, \, T\to T_\infty, \, C\to C_\infty \, \, as \, \, y\to\infty, \tag{5}$$

where u and v denote the velocity components in the x- and y- directions respectively, T is the fluid temperature, g is the acceleration due to gravity, α is the thermal diffusivity, β_T is the coefficient of thermal

expansion, β_C is the coefficient of concentration expansion, σ is the electrical conductivity of the fluid, B_0 is the externally imposed magnetic field strength in the y-direction, ρ is the density of the fluid, T_∞ is the

free stream temperature, C_∞ is the free stream concentration of the species, D_m is the mass diffusivity, c_p is the specific heat capacity, c_s is the concentration susceptibility, T_m is the mean fluid temperature and k_0 is the viscoelastic parameter. Further $a(>0)$, b and $c(>0)$ are constants with $b>0$ for a heated plate $(T_w >$

$T_\infty)$ and $b<0$ for a cooled surface $(T_w < T_\infty)$, respectively.

The governing equations can be transformed by introducing a dimensionless stream functions with the following similarity variables

$$\psi = x\sqrt{a\upsilon}\, f(\eta), \quad \theta(\eta) = \frac{T - T_\infty}{T_w - T_\infty}, \quad \phi(\eta) = \frac{C - C_\infty}{C_w - C_\infty}, \eta = \sqrt{\frac{a}{\upsilon}}\, y. \tag{6}$$

Putting Eq. (6) into Eqs. (2)-(4), we have the following ordinary differential equations

$$F''' + FF'' - F'^2 - K\left(FF^{iv} - 2F'F''' + F''^2\right) - \gamma F' - \delta F' + \lambda\left(\theta + N\phi\right) = 0, \tag{7}$$

$$\theta'' + \Pr \theta' - \Pr \theta F' + Du\phi'' = 0, \tag{8}$$

$$\phi'' + \Pr Le\left(F\phi' - \phi F'\right) + SrLe\,\theta'' = 0, \tag{9}$$

$$F(0) = 0, \quad F'(0) = 1, \quad \theta(0) = 1, \quad \phi(0) = 1,$$
$$F'(\infty) \to 0, \quad F''(\infty) \to 0, \quad \theta(\infty) \to 0, \quad \phi(\infty) \to 0. \tag{10}$$

Here $Pr = \upsilon/\alpha_m$ is the Prandtl number, $Le = \alpha_m/D_e$ is the Lewis number, λ is the constant dimensionless mixed convection parameter, $K(\geq 0)$ is the dimensionless viscoelastic parameter, N is the constant dimensionless concentration buoyancy parameter, γ is the constant dimensionless porosity parameter, δ is the constant dimensionless magnetic field parameter, Du is the Dufour number and Sr is the Soret number, which are defined as

$$\delta = \frac{\sigma B_0^2}{\rho a}, \quad \gamma = \frac{\upsilon}{aK}, \quad \lambda = \frac{Gr_x}{Re_x^2}, \quad K = \frac{k_0 a}{\upsilon}, \quad N = \frac{\beta_C\left(C_w - C_\infty\right)}{\beta_T\left(T_w - T_\infty\right)},$$
$$Du = \frac{D_e k_T\left(C_w - C_\infty\right)}{c_s c_p\left(T_w - T_\infty\right)}, \quad Sr = \frac{D_e k_T\left(T_w = T_\infty\right)}{T_m \alpha_m\left(C_w - C_\infty\right)}, \tag{11}$$

with $Gr_x = g\beta_T\left(T_w - T_\infty\right)x^3/\upsilon^2$ being the local Grashof number and $Re_x = u_w x/\upsilon$ is the local Reynolds number.

III. NUMERICAL PROCEDURE

The set of non-linear ordinary differential equations (7)–(9) with boundary conditions in (10) have been solved numerically by using the Runge–Kutta integration scheme with a modified version of the Newton–Raphson shooting method with γ, K, N, Pr, Le, Du, Sr, δ and λ as prescribed parameters. The computations were done by a program which uses a symbolic and computational computer language MAPLE [18]. A step size of $\Delta\eta = 0.001$ was selected to be satisfactory for a convergence criterion of 10^{-7} in nearly all cases. The value of y_∞ was found to each iteration loop by the assignment statement $\eta_\infty = \eta_\infty + \Delta\eta$. The maximum value of η_∞, to each group of parameters γ, K, N, Pr, Le, Du, Sr, δ and λ is

determined when the values of unknown boundary conditions at $\eta = 0$ not change to successful loop with error less than 10^{-7}.

IV. RESULTS AND DISCUSSION

Here, we assigned physically realistic numerical values to the embedded parameters in the system in order to gain an insight into the flow structure with respect to velocity, temperature and concentration profiles. In all computations we desire the variation of $F', \theta, and\ \phi$ versus η for the velocity, temperature and species diffusion boundary layers. Table (1) and (2) shows the comparison of Hayat et al [16] work with $\delta = 0$ and it is noteworthy that there is an agreement despite the fact that Hayat et al. [12] used HAM which gives a closed form solution. The values of skin friction coefficient, the local Nusselt number and the local Sherwood number for various values of embedded parameters are shown in table (1). It is

clearly seen that $\lambda>0$ corresponds to assisting flow (heated plate), $\lambda<0$ corresponds to opposing flow (cooled plate) and $\lambda=0$ corresponds to forced convection flow, respectively. It must also be noticed that N can take positive values, negative values and N can be zero (mass transfer is absent). We further notice that increasing Pr, Sr and δ parameters leads to an increase in the concentration boundary layer thickness while increasing in λ, Du and Le resulted into shear thinning of the boundary layer. Finally, we observed that the flow field is appreciably influenced by the Dufour and Soret effects.

Table 1 : Computations showing comparison of $-F''(0), -\theta'(0) \, and -\phi'(0)$ with Hayat et al. [12].

									Present	Present	Present	Hayat et al. [16]	Hayat et al. [16]	Hayat et al. [16]
K	γ	λ	N	Pr	Du	Le	Sr	δ	$-F''(0)$	$-\theta'(0)$	$-\phi'(0)$	$-F''(0)$	$-\theta'(0)$	$-\phi'(0)$
0	2	1	-0.2	1	0.1	1	0.2	0	1.4148	0.8657	0.8034	1.4148	0.8657	0.8034
0.2	2	1	-0.2	1	0.1	1	0.2	0	1.2949	0.8865	0.8235	1.2949	0.8865	0.8235
0.4	2	1	-0.2	1	0.1	1	0.2	0	1.2065	0.9030	0.8397	1.2065	0.9030	0.8397
0.1	0	1	-0.2	1	0.1	1	0.2	0	0.7466	1.0023	0.9379	0.7466	1.0023	0.9379
0.1	1	1	-0.2	1	0.1	1	0.2	0	1.0298	0.9417	0.8778	1.0298	0.9417	0.8778
0.1	2	1	-0.2	1	0.1	1	0.2	0	1.3498	0.8767	0.8140	1.3498	0.8767	0.8140
0.1	3	1	-0.2	1	0.1	1	0.2	0	1.5463	0.8435	0.7813	-	-	-
0.1	1	0	-0.2	1	0.1	1	0.2	0	1.3484	0.8551	0.7916	1.3484	0.8551	0.7916
0.1	1	1	-0.2	1	0.1	1	0.2	0	1.0298	0.9417	0.8778	1.0298	0.9417	0.8778
0.1	1	2	-0.2	1	0.1	1	0.2	0	0.7524	0.9937	0.9291	0.7524	0.9937	0.9291
0.1	1	1	-0.5	0.7	0.1	1	0.2	0	1.1261	0.7478	0.6758	1.1261	0.7478	0.6758
0.1	1	1	-0.5	1.2	0.1	1	0.2	0	1.1567	1.0106	0.9545	1.1567	1.0106	0.9545
0.1	1	1	-0.5	1.7	0.1	1	0.2	0	1.1742	1.2151	1.1899	1.1742	1.2151	1.1899
0.1	1	1	-0.5	1	0.3	1	0.2	0	1.1205	0.8155	0.8805	1.1205	0.8155	0.8805
0.1	1	1	-0.5	1	0.5	1	0.2	0	1.0950	0.7103	0.9102	1.0950	0.7103	0.9102
0.1	1	1	-0.5	1	0.7	1	0.2	0	1.0700	0.5975	0.9397	1.0700	0.5975	0.9397
0.1	1	1	-0.5	1	0.1	1.2	0.2	0	1.1344	0.9976	0.9604	1.1344	0.9976	0.9604
0.1	1	1	-0.5	1	0.1	1.5	0.2	0	1.1201	0.9070	1.1082	1.1201	0.9070	1.1082
0.1	1	1	-0.5	1	0.1	1.7	0.2	0	1.1125	0.9030	1.1981	1.1125	0.9030	1.1981
0.1	1	1	-0.5	1	0.1	1.7	0.2	0	1.1125	0.9030	1.1981	1.1125	0.9030	1.1981
0.1	1	1	-0.5	1	0.1	1	0.4	0	1.1296	0.9091	1.0174	1.1296	0.9091	1.0174
0.1	1	1	-0.5	1	0.1	1	0.6	0	1.1475	0.9153	0.8277	1.1475	0.9153	0.8277
0.1	1	1	-0.5	1	0.1	1	0.2	1	1.0760	0.9144	0.8505	-	-	-
0.1	1	1	-0.5	1	0.1	1	0.2	2	1.3831	0.8566	0.7940	-	-	-
0.1	1	1	-0.5	1	0.1	1	0.2	3	1.6472	0.8092	0.7481	-	-	-

Table 2 : Comparison of value of $-\theta'(0)$ for some values of Pr when $\lambda=K=Du=\delta=0$, $\gamma=1$, $N=-0.5$, $Le=1$, $Sr=0.2$

Pr	Hayat et al.[16]	Present results
0.01	0.01977	0.019772
0.72	0.80863	0.808631
1	1.00000	1.000001
3	1.92374	1.923744
10	3.72075	3.720753

a) Velocity Profiles

Figures 1-6 depict the effects of emerging flow parameters on non-dimensional velocity profiles. Figure 1 depicts the influence of Dufour number on the velocity boundary layer and it was observed that increase Dufour number brings a slight increase in the fluid velocity. In figure 2, it is observed that increasing the porosity parameter lead to decrease in the fluid velocity which resulted to velocity boundary layer thinning. Figure 3, It is clearly seen that $\lambda>0$ corresponds to assisting flow (heated plate). Increase in the mixed convection parameter leads to an increase in the fluid velocity. It is clearly seen in figure 4 that the effect of increasing the magnetic field strength on the momentum boundary-layer thickness is illustrated. Increasing this parameter lead to a decrease in the velocity which confirmed with the fact that the magnetic field presents a damping effect on the velocity by creating a drag force that opposes the fluid motion. Figure 5 display the solution of velocity profiles across the boundary layer for different values of dimensionless viscoelastic parameter K and it was observed that increasing the value of K leads to an increase in the fluid velocity and thereby thickening the

velocity boundary layer. Finally, in figure 6, we display the solution of the velocity profiles for various values of the dimensionless concentration buoyancy parameter. If $N < 0$, then it slows down the fluid velocity but if $N > 0$, the fluid velocity increases.

b) *Temperature Profiles*

Figures 7-15 depicts the effects of embedded parameters in the flow on non-dimensional temperature profiles. Figure 7 display the variations of Prandtl number (Pr) on the temperature. The thermal boundary layer thickness is found to decrease upon increasing the Prandtl number. It is reasonable in the sense that larger Prandtl number corresponds to the weaker thermal diffusivity and thinner boundary layer. In figures 8 and 9, we observed that increase in Lewis number (Le) and Soret number (Sr) has little effect on the fluid temperature. Increasing Dufour number (Du) lead to an increase in the fluid temperature (see figure 10). In figure 11, we display the solution of temperature profiles across the boundary layer thickness for different values of dimensionless porosity parameter (γ) and we noticed that increasing this porosity leads to an increase in the fluid temperature. However temperature and the thermal boundary layer thickness increase for large value of γ. The effect of λ on the temperature is analyzed in figure 12. It is observed that temperature and the thermal boundary layer thickness decrease when λ is increased. In figure 13, we display the influence of magnetic parameter (δ) on the temperature of the system. Increasing δ lead to an increase in the fluid temperature which resulted to the thermal boundary layer thickening. Figure 14 depicts the solution of the temperature profiles for various values of dimensionless viscoelastic parameter (K). It is interesting to note that increasing viscoelastic parameter decreases the fluid temperature. Finally, in figure 15, we display the solution of the temperature

profiles for various values of the dimensionless concentration buoyancy parameter N at it was observed that whenever $N > 0$, the thermal boundary layer thickness decreases and increases whenever $N < 0$.

c) *Concentration Profiles*

The effects of embedded parameters on concentration field ϕ are discussed in Figures 16-24. It is clearly seen that the behavior of K and γ on the concentration field is opposite to that of temperature field which is obvious from figures 23 and 20. It is interesting to note that the effects of λ and Pr on the temperature and concentration profiles are similar (Figures 21 and 16). In figure 17, we display the solution of concentration profile for various values of Lewis number (Le). The effect of Lewis number on the concentration profile is as Le gradually increases, this corresponds to the weaker molecular diffusivity and thinner boundary layer thickness. The effect of Dufour and Soret number on the concentration field is found in figures 19 and 18. Increasing Dufour number leads to a small decrease in the concentration boundary layer thickness while increasing the Soret number increases the concentration boundary layer thickness. It is noticed that the behavior of Du and Sr on the temperature and concentration fields is opposite. Similarly, in figure 22, the effect of increasing the imposed magnetic field strength δ on the concentration field is to increase the concentration boundary layer thickness. Finally, in figure 15, we display the solution of the concentration profiles for various values of the dimensionless concentration buoyancy parameter N at it was observed that whenever $N > 0$, the thermal boundary layer thickness decreases and increases whenever $N < 0$ as in the case of the concentration fields.
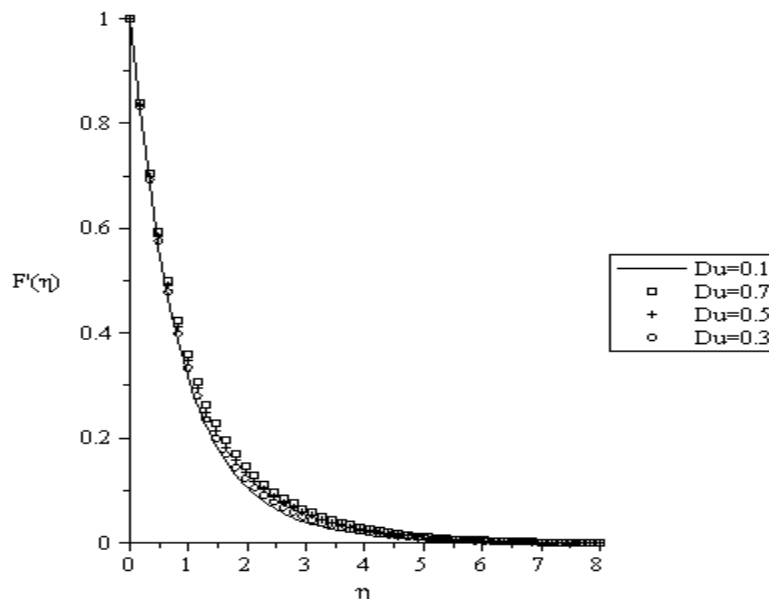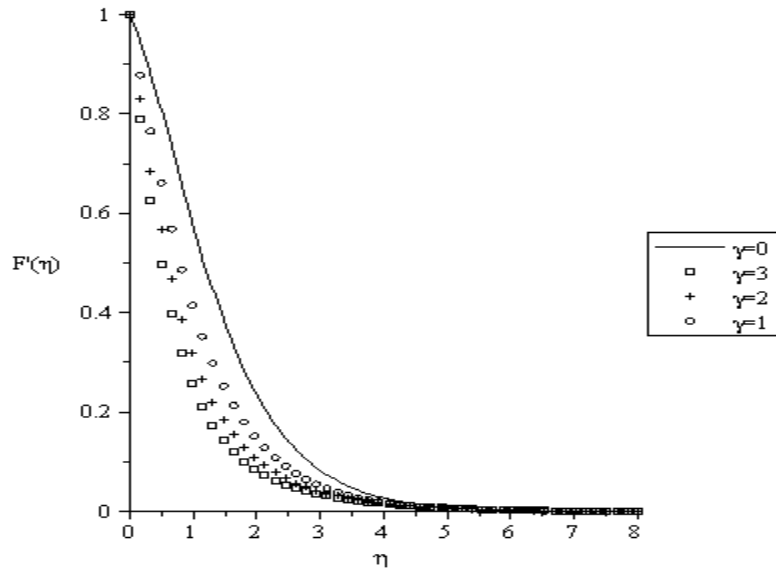

Figure 1 : Velocity profiles for $\gamma=2$, $\lambda=1$, $\delta=0.1$, K=0.1, Sr=0.1, Pr=1, Le=1, N=-0.1

Figure 2 : Velocity profiles for Du=0.1, λ=1, δ=0.1, K=0.1, Sr=0.1, Pr=1, Le=1, N=-0.1

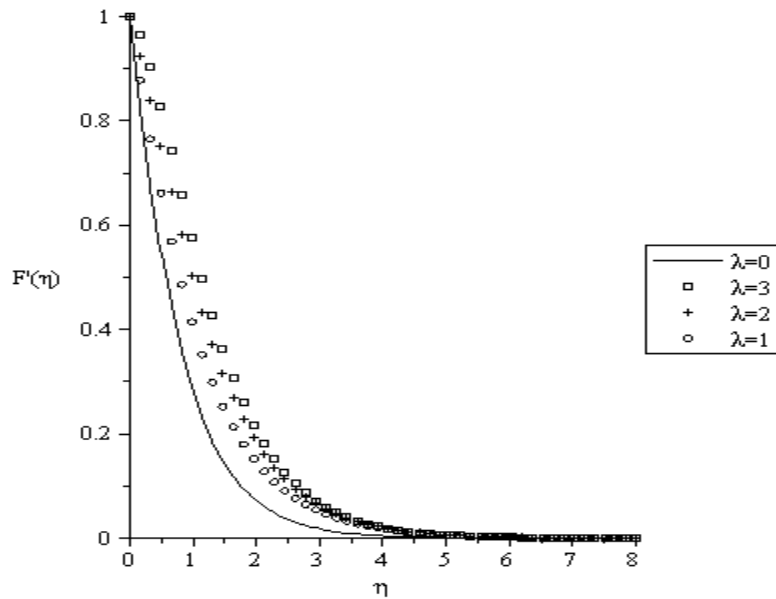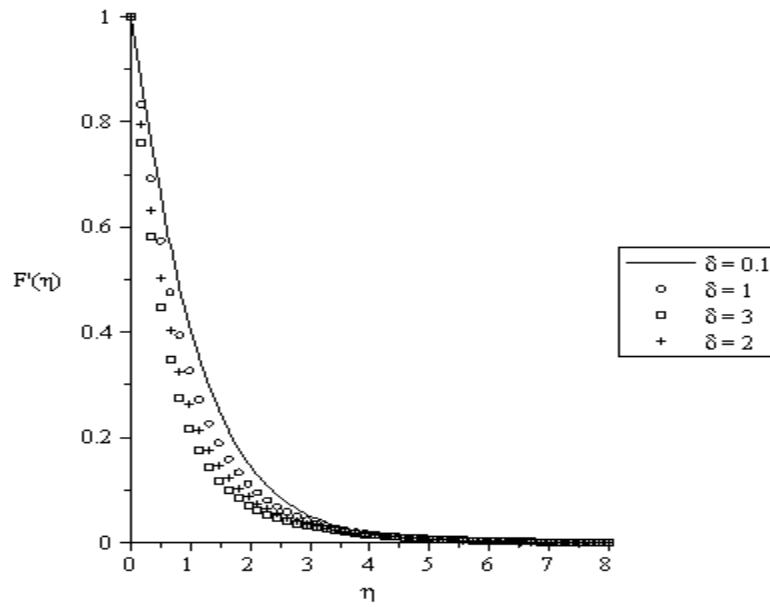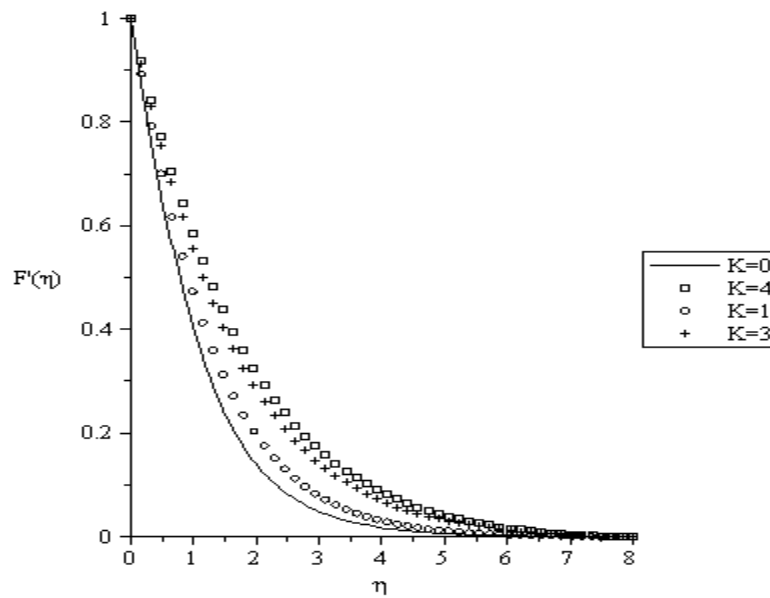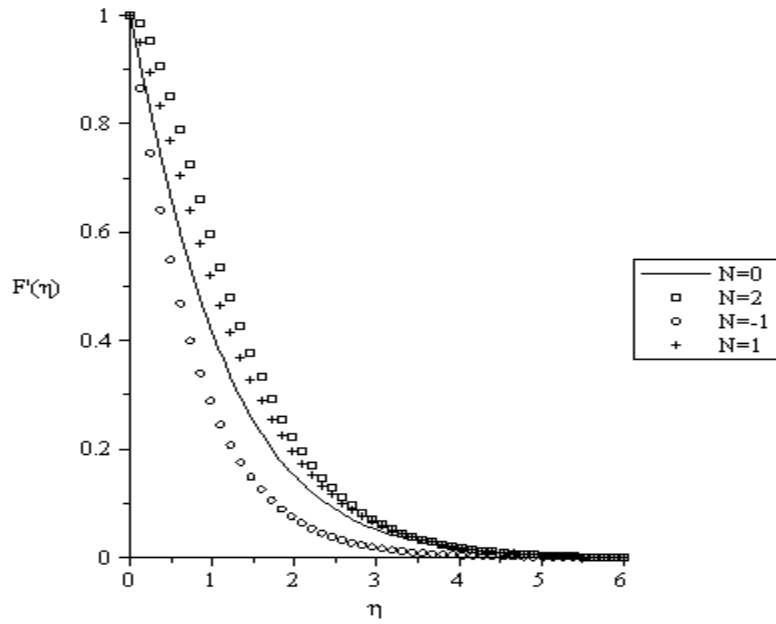*Figure 3 :* Velocity profiles for Du=0.1, γ=1, δ=0.1, K=0.1, Sr=0.1, Pr=1, Le=1, N=-0.1

Figure 4 : Velocity profiles for Du=0.1, γ=1, λ=1, K=0.1, Sr=0.1, Pr=1, Le=1, N=-0.1

Figure 5 : Velocity profiles for Du=0.1, γ=1, λ=1, δ=0.1, Sr=0.1, Pr=1, Le=1, N=-0.1

Figure 6 : Velocity profiles for Du=0.1, γ=1, λ=1, δ=0.1, Sr=0.1, Pr=1, Le=1, K=0.1
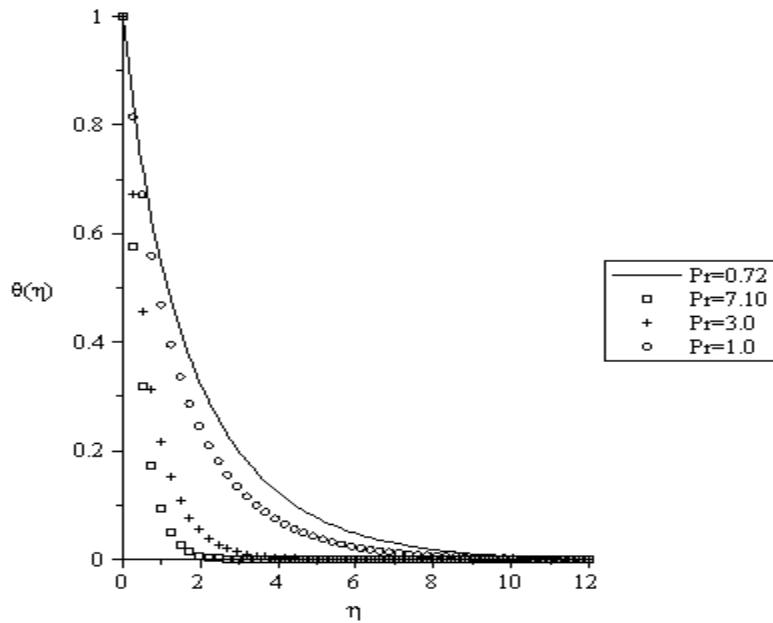
Figure 7 : Temperature profiles for γ=2, λ=1, δ=0.1, K=0.1, Du=0.1, Le=1, Sr=0.7, N=-0.5
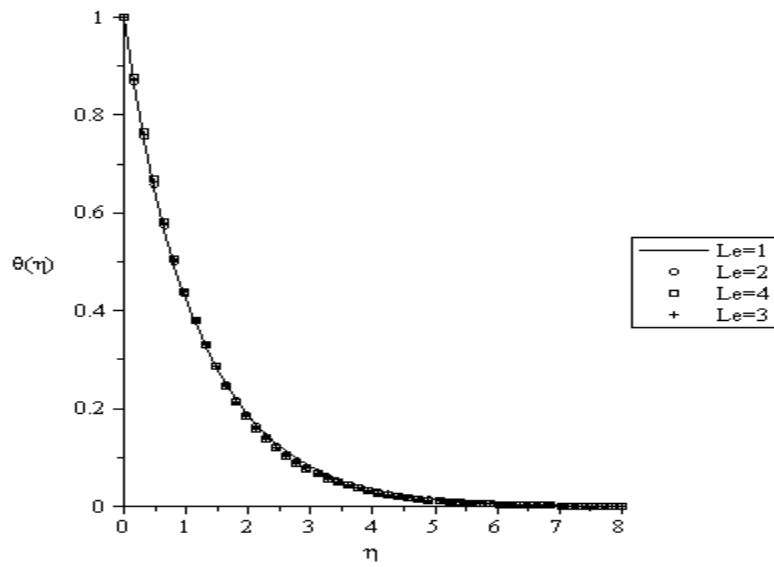
Figure 8 : Temperature profiles for γ=2, λ=1, δ=0.1, K=0.1, Du=0.1, Pr=1, Sr=0.1, N=-0.1

Figure 9 : Temperature profiles for γ=2, λ=1, δ=0.1, K=0.1, Du=0.1, Pr=1, Le=1, N=-0.1

Figure 10 : Temperature profiles for $\gamma=2$, $\lambda=1$, $\delta=0.1$, K=0.1, Sr=0.1, Pr=1, Le=1, N=-0.1
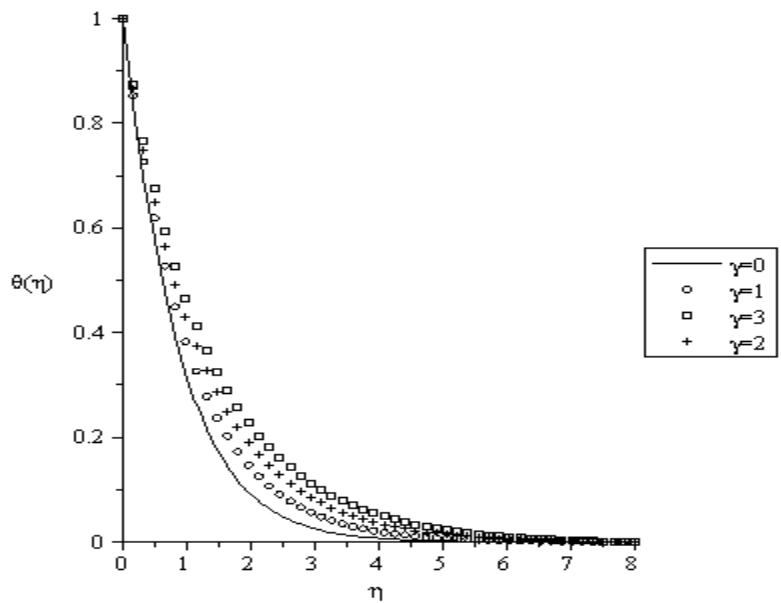
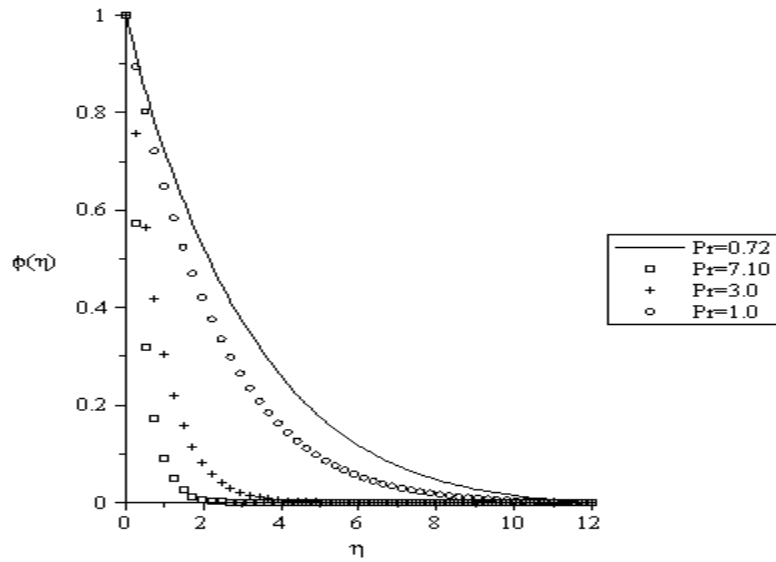*Figure 11 :* Temperature profiles for Du=0.1, $\lambda=1$, $\delta=0.1$, K=0.1, Sr=0.1, Pr=1, Le=1, N=-0.1
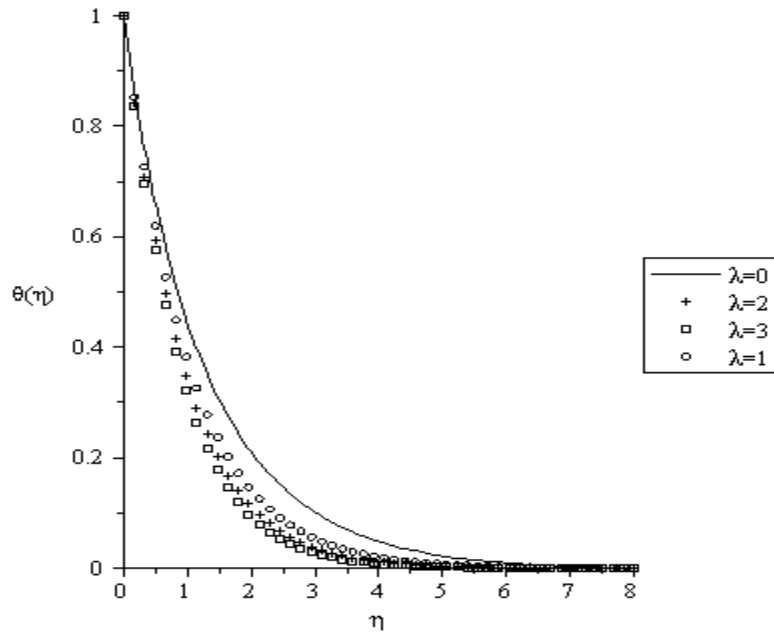
Figure 12 : Temperature profiles for Du=0.1, γ=1, δ=0.1, K=0.1, Sr=0.1, Pr=1, Le=1, N=-0.1
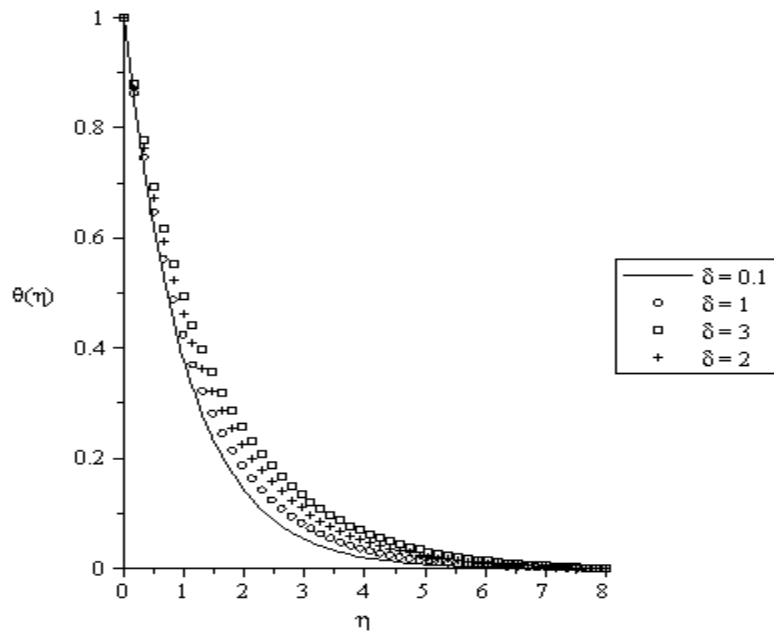
Figure 13 : Temperature profiles for Du=0.1, γ=1, λ=1, K=0.1, Sr=0.1, Pr=1, Le=1, N=-0.1
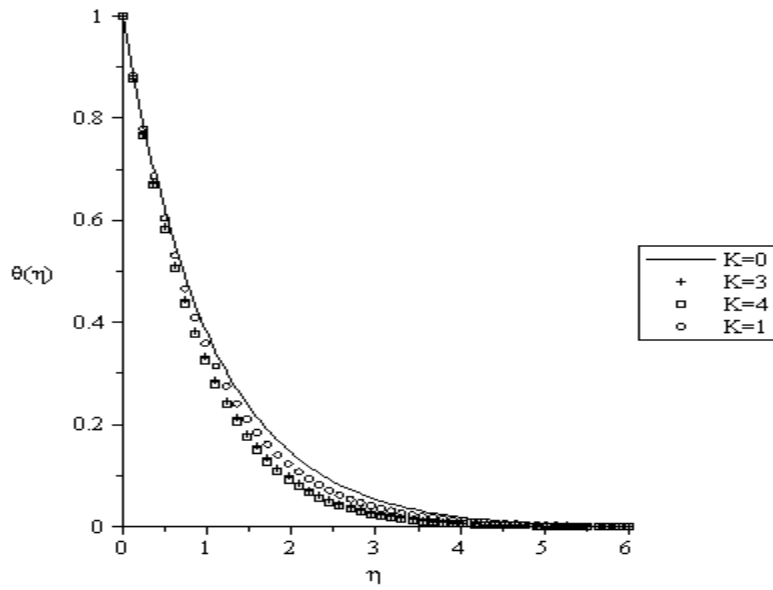
Figure 14 : Temperature profiles for Du=0.1, γ=1, λ=1, δ=0.1, Sr=0.1, Pr=1, Le=1, N=-0.1
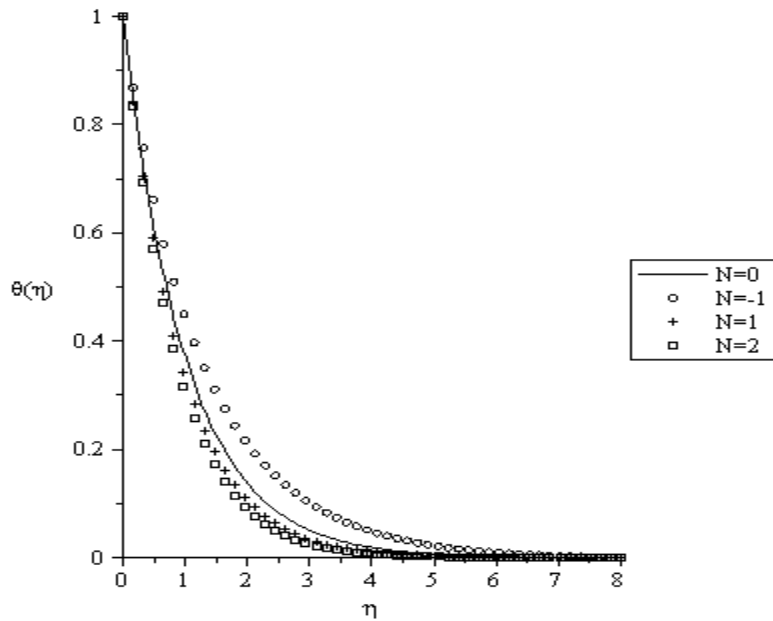
Figure 15 : Temperature profiles for Du=0.1, γ=1, λ=1, δ=0.1, Sr=0.1, Pr=1, Le=1, K=0.1

Figure 16 : Concentration profiles for γ=2, λ=1, δ=0.1, K=0.1, Du=0.1, Le=1, Sr=0.7, N=-0.5
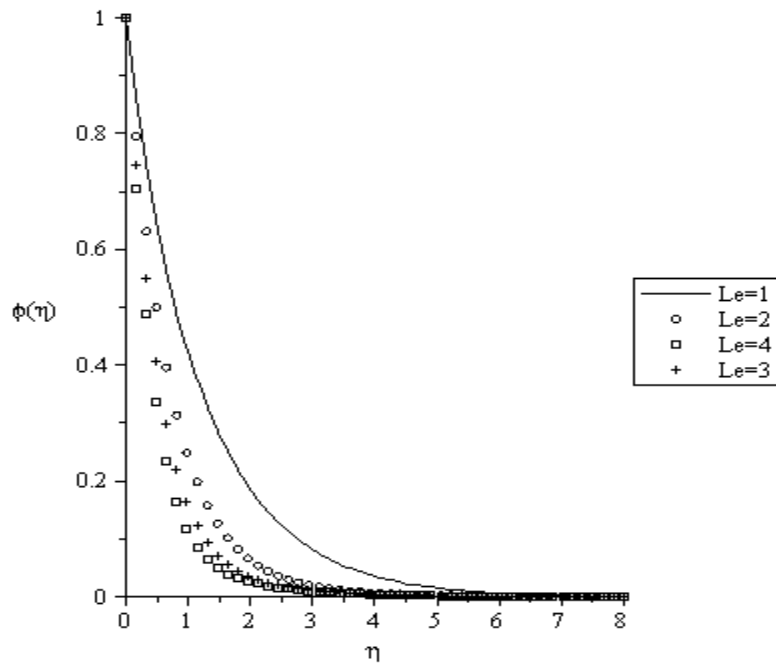
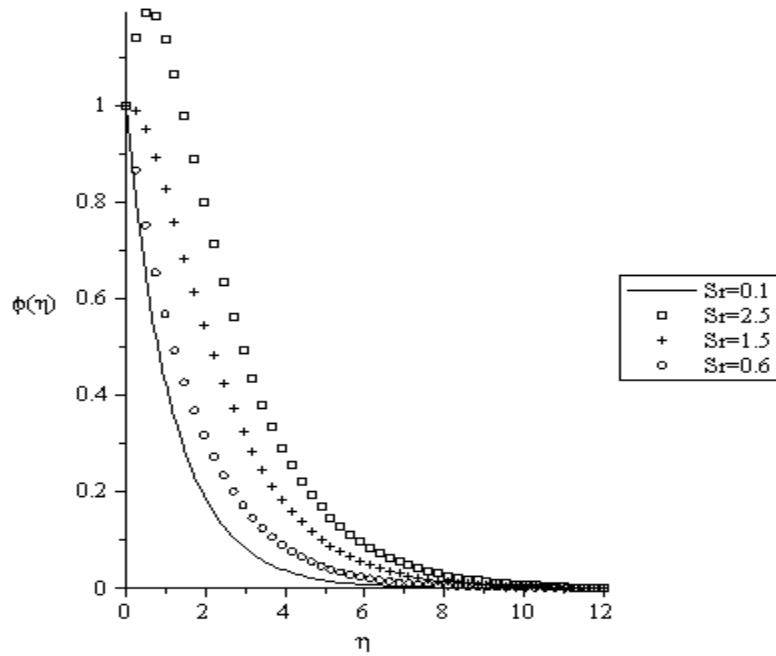*Figure 17 :* Concentration profiles for γ=2, λ=1, δ=0.1, K=0.1, Du=0.1, Pr=1, Sr=0.1, N=-0.1

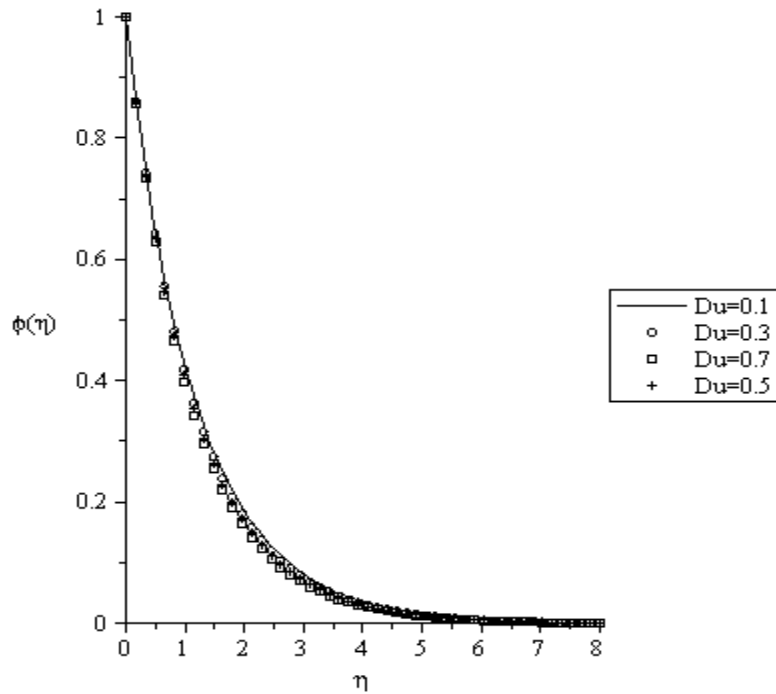Figure 18 : Concentration profiles for $\gamma=2$, $\lambda=1$, $\delta=0.1$, K=0.1, Du=0.1, Pr=1, Le=1, N=-0.1

Figure 19 : Concentration profiles for $\gamma=2$, $\lambda=1$, $\delta=0.1$, K=0.1, Sr=0.1, Pr=1, Le=1, N=-0.1
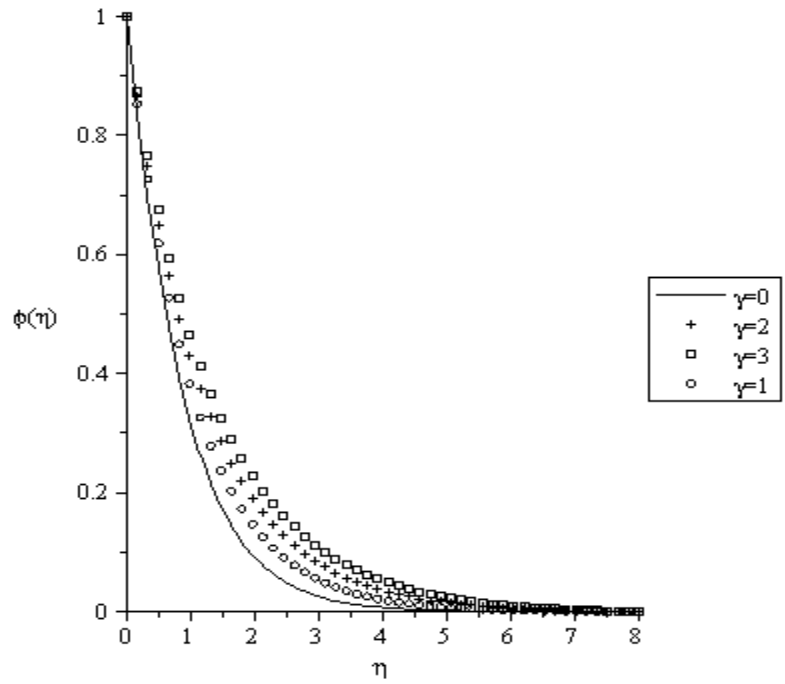
Figure 20 : Concentration profiles for Du=0.1, λ=1, δ=0.1, K=0.1, Sr=0.1, Pr=1, Le=1, N=-0.1

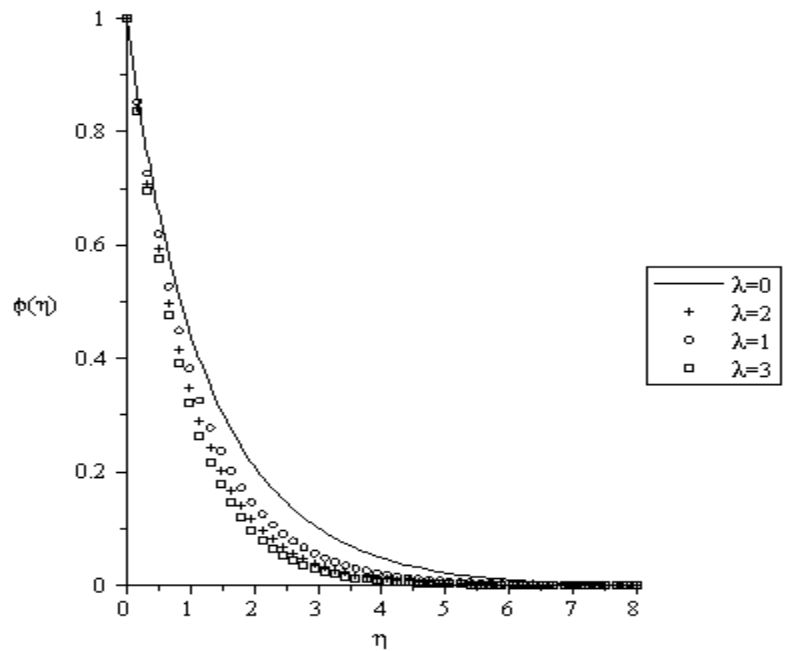*Figure 21 :* Concentration profiles for Du=0.1, γ=1, δ=0.1, K=0.1, Sr=0.1, Pr=1, Le=1, N=-0.1
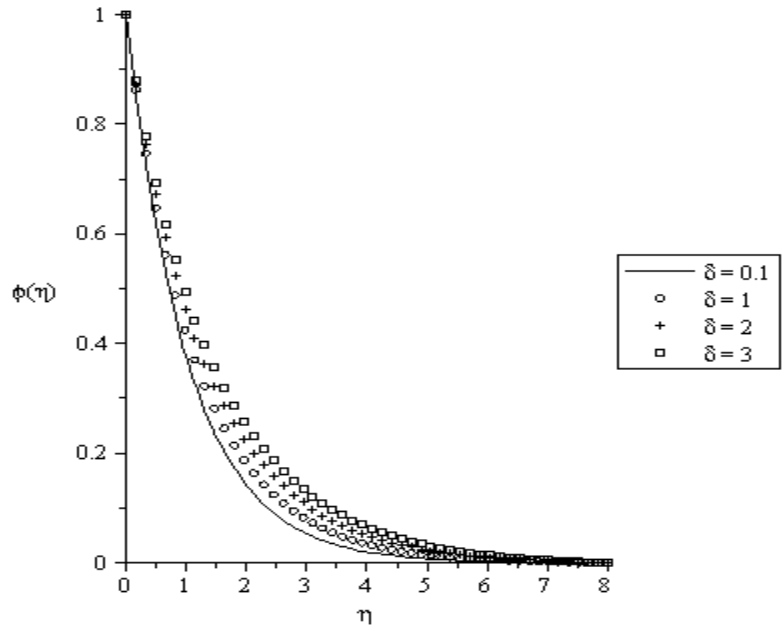
Figure 22 : Concentration profiles for Du=0.1, γ=1, λ=1, K=0.1, Sr=0.1, Pr=1, Le=1, N=-0.1
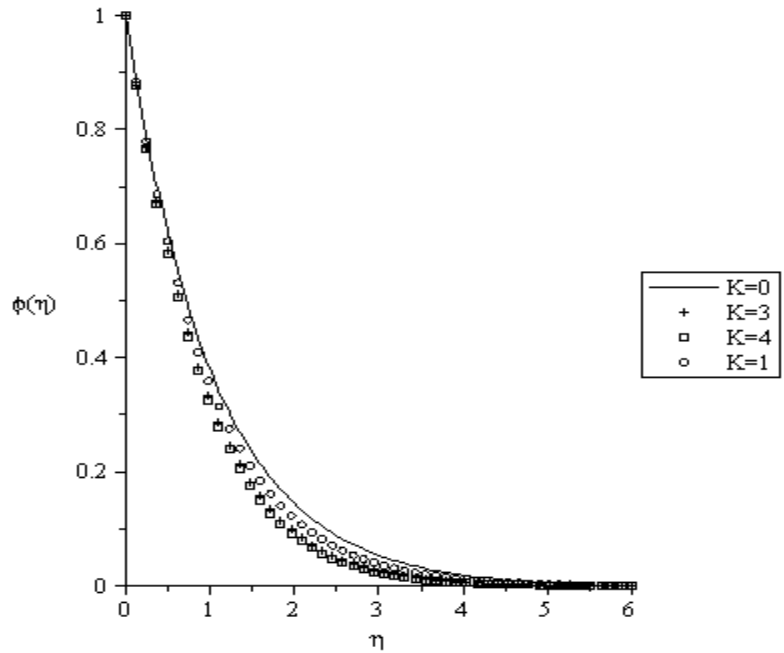
Figure 23 : Concentration profiles for Du=0.1, γ=1, λ=1, δ=0.1, Sr=0.1, Pr=1, Le=1, N=-0.1
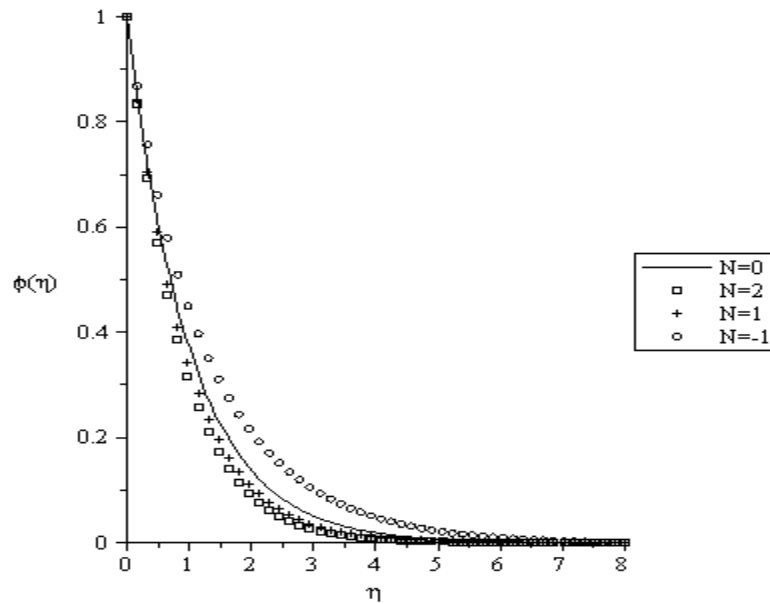
Figure 24 : Concentration profiles for Du=0.1, γ=1, λ=1, δ=0.1, Sr=0.1, Pr=1, Le=1, K=0.1

V. CONCLUSIONS

Thermal-diffusion and diffusion-thermo effects on combined heat and mass transfer on mixed convection boundary layer flow over a stretching vertical surface in a porous medium filled with a viscoelastic fluid in the presence of magnetic field is investigated. The partial differential equations governing the problem have been transformed by a similarity transformation into a system of ordinary differential equations which are solved numerically by using the shooting method with sixth-order of Runge-Kutta technique which are compared with Homotopy Adomian's Decomposition Method (HAM) for special case when magnetic field parameter is zero For fluids of medium molecular weight (H_2, air), profiles of the dimensionless velocity, temperature and concentration distributions are shown graphically for various values of parameters embedded in the flow model. Our results reveal among others that;

- the velocity boundary layer thickness decreases with an increase in dimensionless imposed magnetic field and for dimensionless mixed convection parameter we observed the following. We notice that $\lambda > 0$ corresponds to assisting flow, $\lambda < 0$ corresponds to opposing flow and $\lambda = 0$ corresponds to forced convection flow, respectively.
- the thermal boundary layer thickness increases with a decrease in K and λ and the thermal boundary layer increases as *Le, Du, γ* and *δ* increases.
- the local skin-friction and the rate of heat transfer at the plate increases as *Sr, γ, δ* and *N <0*

increases and decreases as *Pr, Le, Du, λ, K* and *N > 0* increases.

REFERENCES REFERENCES REFERENCIAS

1. Chakrabarti A, Gupta AS. Hydromagnetic flow and heat transfer over a stretching sheet. Q Appl Math 1979; 37:73-8.
2. Sakiadis BC. Boundary layer behavior on continuous solid surfaces I. Boundary layer equations for two-dimensional and axisymmetric flow. AICHE J 1961;7:26-8.
3. Chiam TC. Hydrodynamic flow over a surface stretching with a power law velocity. Int J Eng Sci 1995;33:429-35.
4. Eckert ER, Drake RM. Analysis of heat and mass transfer. New York: McGraw Hill; 1972.
5. Platten JK, Legros JC. Convection in liquids. New York: Springer; 1984.
6. Benano-Melly LB, Caltagirone JP, Faissat B, Montel F, Costeseque P. Modeling Soret coefficient measurement experiments in porous media considering thermal and solutal convection. Int J Heat Mass Transfer 2001; 44:1285-97.
7. Alam M.S., Rahman M.M., Dufour and Soret effects on mixed convection flow past a vertical porous flat plate with variable suction. Nonlinear Analysis: Modelling and Control, 2006, Vol. 11, No. 1, 3-12.
8. Gaikwad S.N., Malashetty M.S., Prasad K. Rama, An analytical study of linear and nonlinear double diffusive convection with Soret and Dufour effects in couple stress fluid. International Journal of Non-Linear Mechanics 42 (2007) 903-913.
9. Emmanuel Osalusi, Jonathan Side, Robert Harris,

Thermal-diffusion and diffusion-thermo effects on combined heat and mass transfer of a steady MHD convective and slip flow due to a rotating disk with viscous dissipation and Ohmic heating. International Communications in Heat and Mass Transfer 35 (2008) 908-915.

10. Beg Anwar O., Bakier A.Y., Prasad V.R., Numerical study of free convection magnetohydrodynamic heat and mass transfer from a stretching surface to a saturated porous medium with Soret and Dufour effects. Computational Material Science 46 (2009) 57-65.

11. Nithyadevi N., Yang Ruey-Jen. Double diffusive natural convection in a partially heated enclosure with Soret and Dufour effects. International Journal of Heat and Fluid Flow, 2009 (In Press).

12. Olanrewaju Philip Oladapo, Dufour and Soret Effects of a Transient Free Convective Flow with Radiative Heat Transfer Past a Flat Plate Moving Through a Binary Mixture. Pasific Journal of Science and Technology, Vol. 11. No. 1. May 2010 (Spring).

13. Emmanuel Osalusi, Jonathan Side, Robert Harris. Thermal-diffusion and diffusion-thermo effects on combined heat and mass transfer of a steady MHD convective and slip flow due to a rotating disk with viscous dissipation and Ohmic heating. International Communications in Heat and Mass Transfer 35 (2008) 908-915.

14. Anwar Beg O, Bakier AY, Prasad VR. Numerical study of free convection magnetohydrodynamic heat and mass transfer from a stretching surface to a saturated porous medium with Soret and Dufour effects. Computational Materials Science 46 (2009) 57-65.

15. Ahmed AA. Similarity solution in MHD: Effects of thermal diffusion and diffusion thermo on free convective heat and mass transfer over a stretching surface considering suction or injection. Commun Nonlinear Sci Numer Simulat 14 (2009) 2202-2214.

16. Hayat T, Mustafa M, Pop I. Heat and mass transfer for Soret and Dufour's effect on mixed convection boundary layer flow over a stretching vertical surface in a porous medium filled with a viscoelastic fluid. Commun Nonlinear Sci Numer Simulat 15 (2010) 1183-1196.

17. Tsai R, Huang JS. Heat and mass transfer for Soret and Dufour's effects on Hiemenz flow through porous medium onto a stretching surface. Int J Heat Mass Transfer 2009; 52:2399-406.

18. A. Heck, Introduction to Maple, 3rd Edition, Springer-Verlag, (2003).